

# Structural and Optical Properties of Aliovalent Vanadium Substituted TiO<sub>2</sub>

Nasima Khatun<sup>1, a)</sup>, Saurabh Tiwari<sup>1, b)</sup>, Ruhul Amin<sup>1, c)</sup>, Sajal Biring<sup>2, d)</sup> and Somaditya Sen<sup>1, 2, e)</sup>

<sup>1</sup> Indian Institute of Technology Indore, Khandwa Road, Indore-453552, India

<sup>2</sup> Ming Chi University of Technology, New Taipei City -24301, Taiwan

a) nasima.khatunf7@gmail.com

b) phd1501181003@iiti.ac.in

c) ruhulamin.phys@gmail.com

d) biring@mail.mcut.edu.tw

e) Corresponding author: sens@iiti.ac.in

**Abstract.** Vanadium substituted TiO<sub>2</sub> samples are prepared by modified sol-gel process. X-ray diffraction (XRD) pattern and Raman spectra for all the samples reveal pure tetragonal phases of TiO<sub>2</sub>. Rutile percentage calculated from XRD pattern and Raman spectra follow a similar trend and signify that vanadium substitution promotes phase transformation from anatase to rutile. Due to aliovalent V substitution, donor levels are formed in the bandgap which is responsible for bandgap reduction.

**Keywords:** Sol-gel, Phase transition, bandgap

## INTRODUCTION

TiO<sub>2</sub> is one of the most investigated semiconducting materials because of its tunable bandgap and high chemical stability. Nontoxicity and low cost of TiO<sub>2</sub> give it a special importance in applications field. It is mainly used in photocatalysis, dye-sensitized solar cell, gas sensor, environmental purification, paint, energy storage device etc.<sup>1-3</sup>. It has three phases of crystallinity: anatase, brookite, and rutile<sup>4</sup>. At lower temperature, anatase is the stable crystal structure due to its lower surface free energy than rutile. Rutile is the most thermodynamically stable structure at higher temperature. Synthesis of brookite is very difficult due to its complicated crystal structure. With increasing temperature ( $\geq 600$  °C) both the metastable phases (anatase and brookite) are irreversibly converted into stable rutile phase. Phase transformation from anatase to rutile (A→R) depends on several factors like synthesis methods, temperature, and atmosphere of calcination, presence of impurity, strain and most importantly doping with different elements<sup>1, 5-7</sup>.

Properties of any materials are highly correlated with its crystal structure. Depending on different crystal structure of TiO<sub>2</sub>, it has different physical and chemical properties. It is a well-known wide bandgap n-type semiconductor (3.2 eV for anatase and 3.00 eV for rutile)<sup>8</sup>. Solar spectrum contains 5% UV light, while 45% is visible light. To use this wide range of visible light, researchers are trying to tune the bandgap of TiO<sub>2</sub> in visible region. This tuning was done by several processes such as synthesis method, inducing strain, doping with foreign elements like Si, Mo, Sn, Fe, Ru, Ge, Pb, Al, Co etc.<sup>9-11</sup>. Doping with foreign elements is the easiest way to tune the bandgap of TiO<sub>2</sub>. Here, aliovalent Vanadium has been chosen to see its effect on structural phase transition (A→R) and optical property of TiO<sub>2</sub>.

In this work, effect of different Vanadium concentration on crystal structure and optical property of TiO<sub>2</sub> have been presented. Phase transformation is confirmed by both XRD pattern and Raman spectra. Bandgap of the samples is calculated by diffuse reflectance spectroscopy (DRS) measurement.

## EXPERIMENTAL

V doped TiO<sub>2</sub> samples (Ti<sub>1-x</sub>V<sub>x</sub>O<sub>2</sub>: TV0 ( $x=0.00$ ), TV1 (0.01), TV3 (0.03), and TV6 (0.06)) were prepared by modified sol-gel process. This particular sol-gel process is described in our previous report<sup>12</sup>. After decarburization and denitrification at 450 °C for 4h, the samples were heat treated at an elevated temperature 600 °C for 4h in step size of 50 °C are taken for this report.

Structural analysis is done by Bruker D2 phaser diffractometer ( $\lambda = 1.54 \text{ \AA}$ ). Vibrational modes are analyzed by Raman spectroscopy (HORIBA JobinYvon LabRAM HR) using a laser of wavelength 488 nm. Diffuse reflectance spectroscopy (DRS) measurements are carried out by Ocean Optics USB-2000 spectrometer.

## RESULTS AND DISCUSSION

XRD pattern of the samples (Figure 1.(a)) revealed only dominating tetragonal phases of TiO<sub>2</sub> (anatase and rutile). No secondary phase related to V, Ti and O compound have been detected. TV0 and TV1 show mixed phase of anatase and rutile, whereas TV3 almost transform into rutile phase and TV6 completely converted into rutile phase. Spurr and Mayers equation<sup>13</sup> is used to calculate the anatase (A%) and rutile (R%) percentage present in the samples (A%:R%=70.3:29.7 (TV0), 63.7:36.3 (TV1), 2.50:97.5 (TV3), and 0:100 (TV6) respectively). Hence, it is observed that with increasing V concentration rutile percentage increases in the sample. From literature<sup>14</sup>, it was observed that V ions properly substitute Ti ions in TiO<sub>2</sub>. In anatase phase, V ions present in the samples are mostly in 5+ valence state, while in rutile it is in both 5+ and 4+ valence states<sup>12, 15</sup>. Unit cell volume of anatase TiO<sub>2</sub> decreases because V<sup>5+/4+</sup> (VI-0.68 Å/0.65 Å) both have smaller ionic radius than Ti<sup>4+</sup> (VI-0.745 Å) and this lattice contraction helps to influence phase transition. Hence, V substitution promotes the phase transformation of TiO<sub>2</sub>.

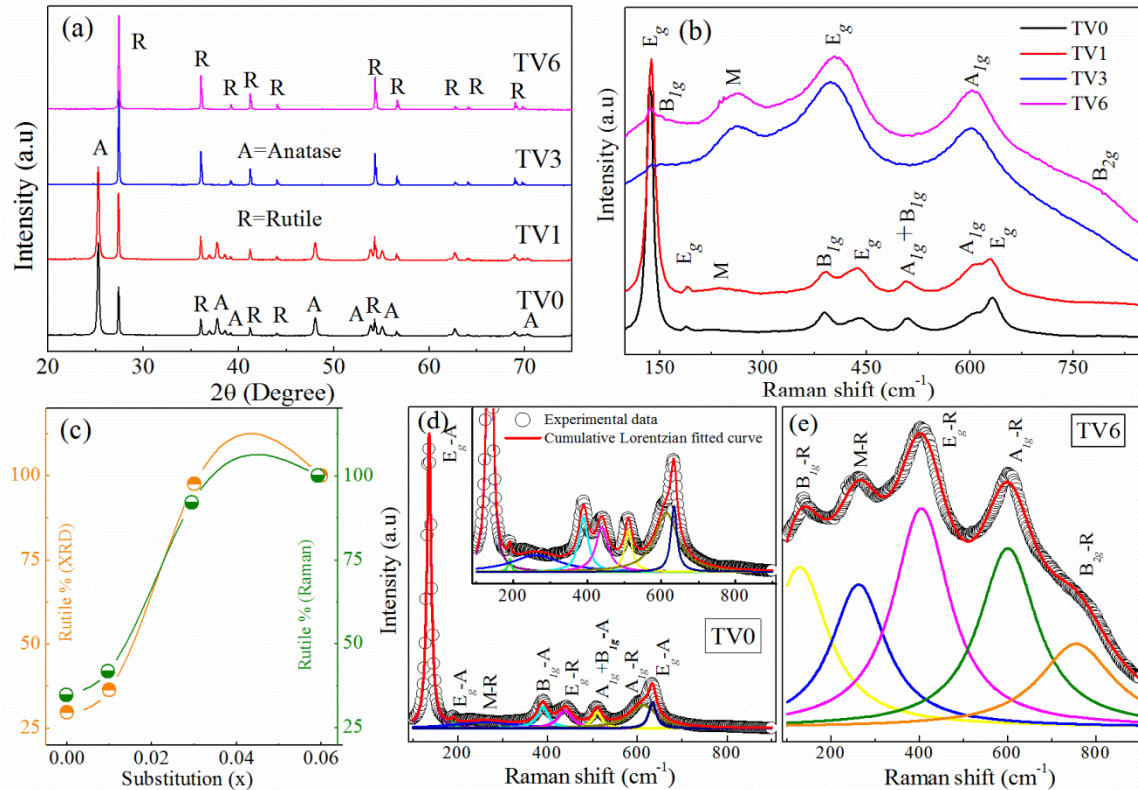


FIGURE 1.(a) XRD pattern and (b) Raman spectra of all TV samples heated at 600 °C. (c) Variation of rutile % from both XRD and Raman spectra, (d) and (e) Lorentzian fitting of TV0 and TV6 samples.

Raman spectroscopy is a very efficient tool to assure phases of any material. Room temperature (RT) Raman spectra of all the samples are shown in Figure 1.(b). From literature, it was observed that anatase has six Raman active modes (three E<sub>g</sub> mode at 144, 197 and 639 cm<sup>-1</sup>, two B<sub>1g</sub> mode at 399 and 519 cm<sup>-1</sup>, one A<sub>1g</sub> at 513 cm<sup>-1</sup>)<sup>16</sup>

whereas rutile has four Raman active modes ( $B_{1g}$ -143 $\text{cm}^{-1}$ ,  $E_g$ -447 $\text{cm}^{-1}$ ,  $A_{1g}$ -612 $\text{cm}^{-1}$ , and  $B_{2g}$ -826  $\text{cm}^{-1}$ ) and one multiphonon mode ( $M$ -240  $\text{cm}^{-1}$ )<sup>17</sup>. It was observed that all the vibrational modes (Figure 1.(b)) correspond to anatase and rutile phases of pure  $\text{TiO}_2$ . In case of visible Raman spectra,  $B_{1g}$  (399  $\text{cm}^{-1}$ ) of anatase and  $E_g$  (447  $\text{cm}^{-1}$ ) of rutile are very sensitive modes. Here, wavelength of laser used for Raman measurement is 488 nm which is in visible region. Hence, area under the curve of  $B_{1g}$  ( $A_A$ ) mode and  $E_g$  ( $A_R$ ) mode are used to calculate the weight ratio of rutile to anatase<sup>18</sup>. For calculation of the area under  $B_{1g}$  and  $E_g$  modes, Raman spectra of all samples fitted using Lorentzian function. Figure 1. (d and e) show fitted Raman spectra of TV0 and TV6. This also shows that there is no impurity related to Ti, V and O compounds. Rutile % calculated from Raman spectra is consistent with XRD result (Figure 1.(c)). Hence, both XRD pattern and Raman spectra confirmed that V substitution promotes the phase transformation (A $\rightarrow$ R).

DRS measurement has been carried out to see the effect of V substitution on bandgap and related changes at the absorption edge of the samples. Tauc plot is being used  $((F(R))h\nu)^{\frac{1}{n}} = A(h\nu - E_g)$  to calculate the bandgap; Where  $F(R) = (1-R)^2/2R$  is the KubelkaMunk function,  $h$  is Planck's constant,  $\nu$  is the frequency of illumination,  $E_g$  is the band gap and  $A \sim$  proportionality constant. Unit less parameter 'n' determines the type of bandgap;  $n=2$  for indirect and  $n=1/2$  for direct bandgap semiconductor.  $\text{TiO}_2$  has been reported to have two types of bandgap indirect (anatase) and direct (rutile)<sup>4</sup>. For TV0 and TV1 as the anatase phase dominates, bandgap is calculated considering the samples as an indirect bandgap semiconductor. Similarly for TV3 and TV6 as rutile phase dominates, bandgap is calculated considering the samples as a direct bandgap semiconductor.

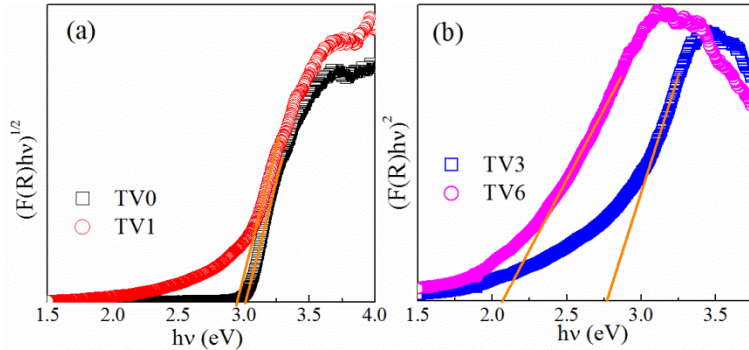


FIGURE 2.(a) Shows RT absorption spectra of TV0 and TV1. (b) TV3 and TV6 respectively.

Redshift in the absorption edge has been observed for all the samples with increasing V substitution along with the decrease in sharpness of the absorption edge. V substitution in  $\text{TiO}_2$  creates donor level just below the conduction band which thereby decreases the effective bandgap of  $\text{TiO}_2$ <sup>19</sup>.  $\text{V}^{4+}$  takes deeper region than  $\text{V}^{5+}$  below the conduction band<sup>20</sup>. For pure  $\text{TiO}_2$  (TV0) bandgap is 3.06 eV and with increasing V substitution bandgap decreases to 2.07 eV for TV6. V present in the sample have both 5+ and 4+ valence states and at higher substitution presence of  $\text{V}^{4+}$  is more than  $\text{V}^{5+}$  due to more rutile%. Hence, with increasing V substitution bandgap decreases and it may absorb visible light of sunlight which is good for visible light photocatalysis application and other optoelectronic applications.

## CONCLUSION

V doped  $\text{TiO}_2$  samples are prepared by modified sol-gel processes. At lower substitution, samples show mixed phase, while at higher substitution samples converted into rutile phase which indicates vanadium substitution promotes the phase transformation. Rutile% present in the samples is confirmed by both XRD pattern and Raman spectra. Due to aliovalent V substitution, donor levels are formed in the bandgap which is responsible for bandgap decrement.

## ACKNOWLEDGMENTS

The authors are thankful to Indian Institute of Technology Indore for providing all research related facilities and especially SMART group of IIT Indore for their valuable discussions.

## REFERENCES

1. D. A. H. Hanaor and C. C. Sorrell, *J. Mater. Sci.* **46** 855-874 (2010).
2. M. Zukalova, A. Zukal, L. Kavan, M. K. Nazeeruddin, P. Liska and M. Gratzel, *Nano Lett.* **5** 1789-1792 (2005).
3. T. Luttrell, S. Halpegamage, J. Tao, A. Kramer, E. Sutter and M. Batzill, *Sci. Rep.* **4**, 4043 (2014).
4. J. Zhang, P. Zhou, J. Liu and J. Yu, *Phys. Chem. Chem. Phys.* **16** 20382-20386 (2014).
5. T. Mitsuhashi and O. J. Kleppa, *J. Am. Ceram. Soc.* **62** 356-357 (1979).
6. N. Khatun, S. Tiwari, C. P. Vinod, C.-M. Tseng, S. Wei Liu, S. Biring and S. Sen, *J. Appl. Phys.* **123** 245702 (2018).
7. N. Khatun, R. Amin, Anita and S. Sen, *AIP Conf. Proc.* **1953**, 040028 (2018).
8. B. Buchholz, H. Haspel, Á. Kukovecz and Z. Kónya, *CrystEngComm* **16** 7486 (2014).
9. W. Choi, A. Termin and M. R. Hoffmann, *J. Phys. Chem.* **98** 13669-13679 (1994).
10. R. Long, Y. Dai, G. Meng and B. Huang, *Phys. Chem. Chem. Phys.* **11** 8165-8172 (2009).
11. Anita, A. K. Yadav, N. Khatun, S. Kumar, C. M. Tseng, S. Biring and S. Sen, *J. Mater. Sci.: Mater. Electron.* **28** 19017-19024 (2017).
12. N. Khatun, E. G. Rini, P. Shirage, P. Rajput, S. N. Jha and S. Sen, *Mater. Sci. Semicon. Proc.* **50** 7-13 (2016).
13. R. A. Spurr and H. Myers, *Anal. Chem.* **29** 760-762 (1957).
14. W. Avansi, R. Arenal, V. R. de Mendonça, C. Ribeiro and E. Longo, *CrystEngComm* **16** 5021 (2014).
15. N. Khatun, Anita, P. Rajput, D. Bhattacharya, S. N. Jha, S. Biring and S. Sen, *Ceram. Int.* **43** 14128-14134 (2017).
16. T. Ohsaka, *J. Phys. Soc. Jpn.* **48** 1661-1668 (1980).
17. S. P. S. Porto, P. A. Fleury and T. C. Damen, *Phys. Rev.* **154** 522-526 (1967).
18. P. K. M. Anpo, Masakazu Anpo, and Prashant V. Kamat, Springer-Verlag New York, 153-184 (2010).
19. T. Umeyashiki, T. Yamaki, H. Itoh and K. Asai, *J. Phys. Chem. Solids* **63** 1909-1920 (2002).
20. A. Y. Choi and C.-H. Han, *J. Nanosci. Nanotechnol.* **14** 8070-8073 (2014).